Cell Categories and K-Nearest Neighbor Algorithm Based Decoding of Primary Motor Cortical Activity during Reach-to-Grasp Task

Yangyang Guo, Wei Li , Jiping He, *Senior Member, IEEE*

***Abstract*—Neural decoding is a procedure to acquire intended movement information from neural activity and generate movement commands to control external devices such as intelligent prostheses. In this study, monkey Astra was trained to accomplish a 3-D reach-to-grasp task, and we recorded neural signals from its primary motor cortex (M1) during the task. The task-related cells were divided into four classes based on their correlation with two movement parameters: movement direction and orientation. We adopted the simple k-nearest neighbor (KNN) algorithm as the classifier, and chose cells from appropriate cell classes for movement parameter decoding. Cell classification was shown improving decoding accuracy with relatively less cells, even during movement planning stage (CRT). High decoding accuracy before movement actually performed is of great significance for intelligent prostheses control, and provides evidence that M1 is more than accepting ready-made movement commands but also participating in movement planning. We also found that population of task-related cells in M1 had a preference for specific direction and orientation, and this preference was more significant when it came to population of direction-related cells and orientation-related cells.**

I. Introduction

A large number of people are suffering from physical disabilities, and reconstruct disabled motor functions, especially hand functions, is of great significance to increasing these patients' quality of life. A kind of intelligent prosthesis with good performance of recognizing users' movement intentions and implementing corresponding movement commands has been paid great attention.

Stable and reliable signals are needed in order to acquire accurate motion intentions from the subjects. The widespread adoption of EMG has been under restrictions of low data volume and dependence on non-atrophied muscles [1]. An EEG-based brain-machine interface (BMI) requires users concentrating on motor imagery [2]. Neural signals from cerebral cortex could provide relatively accurate motor and sensory information, and have been used to control cursor movement [3], operate mechanical arm for self-feeding [4], and command a robotic arm to perform a reach-and-grasp task [5]. Implantation of electrodes in peripheral nerve, carrying a lower risk of infection than cortical implantation, has been used to extract neural commands to control prosthetic hands [6].

In this study, we recorded neural signals from the primary motor cortex (M1) of non-human primate. It has been a generally accepted point that M1 plays a vital role in reaching and grasping movement or such volitional motor control [7]. Compared to M1 which executes motor commands to control spinal circuitry activity, the dorsal premotor cortex (PMd) is deemed to play a higher-level role in movement planning [8]. However, M1 has been proven more than an execution system, but also involving in planning of complex behaviors [9].

A lot of decoding algorithms have been applied in prosthetic control system in recent years, such as the maximum-likelihood (ML) approach [10], state-space model [11], support vector machine (SVM), artificial neural network (ANN) and some other nonlinear approaches. Here we used k-nearest neighbor (KNN) algorithm as the classifier for its simplicity and rapidity, despite of its susceptibility to the sample size. We classified the task-related cells into four categories based on their correlation with movement direction and orientation, utilized the average firing rates of randomly chosen cells during both movement planning and execution as the feature vectors for KNN classifier and achieved fairly good decoding accuracy even based on cortical activity during movement planning. Our results implied M1 indeed played a more crucial role in planning phase than it was thought of. Finally we investigated the tuning preference of related cells and discovered that cells in M1 of the monkey on the mission had a preference for some specific movement direction and orientation.

II. METHODOLOGY

A. Experimental Description and Data Collection

The experiment apparatus and design has been described in detail in [12]. The Institutional Animal Care and Use Committee approved the behavioral paradigm, surgical procedures and general animal care.

There were two rectangular targets with touch sensors on both sides and a central holding pad in the apparatus. Every target could be rotated in three different orientations (45º, 90º, 135º). Monkey Astra was trained to reach and grasp the indicated target with a specific orientation using its right hand. Every successful trial contained four main epochs: from central holding pad hit to one target light on (CHT); from target light on to central pad release (CRT); from central pad release to target hit (MT); from target hit to target release

Resrach supported by National Natural Science Funds of China (60905024, 61233015), and 973 Project of China (2013CB329506).

Yangyang Guo and Wei Li are with the Neural Interface & Rehabilitation Technology Research Center, Huazhong University of Science and Technology, Wuhan, China.

Jiping He is with the Center for Neural Interface Design, Harrington Department of Bioengineering, Arizona State University, Tempe, AZ 85287, USA. He is also with the Neural Interface & Rehabilitation Technology Research Center, Huazhong University of Science and Technology, Wuhan, China (phone: +86-27-87793916; fax: +86-27-87793916; e-mail: jiping.he@asu.edu).

978-1-4244-7929-0/14/$26.00 ©2014 IEEE

(THT). Here we focus our attention on movement planning phase (CRT) and movement execution phase (MT).

A recording-chamber was implanted in M1 of monkey Astra, and five independent microelectrodes (Thomas Recording, Germany) were used for neural activity recording. The depth of each electrode was changed after a complete set, which consisted of 108 successful trials, with 18 trials to each orientation of each target. Figure 1 showed the locations of the recorded neurons.

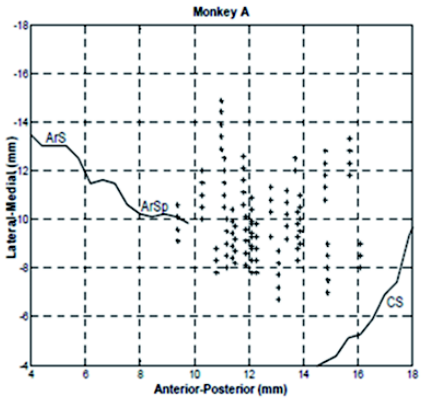

Figure 1. Electrode penetration locations of monkey Astra based on the chamber's coordinates. Each cross represents an electrode penetration. ArS: arcuate sulcus, ArSp: arcuate sulcus spur, CS: central sulcus.

B. Signal Analysis

In this study, we focused on the motor cortical activity during movement planning phase (CRT) and execution phase (MT). Single cells were isolated offline (Offline Sorter; Plexon, Inc). For each single cell, the average firing rate during CHT was defined as the baseline and the cell was regarded task-related during CRT or MT if its firing rate during each epoch was significantly higher than the baseline (t-test, $p<0.05$). Further analysis was based on the task-related cells during different epochs respectively. Epoch firing rates of task-related cells were grouped by movement direction (2 levels) and target orientation (3 levels). A two-way analysis of variance (ANOVA, $p<0.01$) was utilized to determine whether a cell's discharge rate was significantly modulated by movement direction, or target orientation, or both of them, or neither. According to the results of ANOVA ($p<0.01$), we divided task-related cells during each epoch (CRT and MT) into four classes: direction-only cells (only tuning movement direction), orientation-only cells (correlated only with target orientation), both-related cells (correlated with both direction and orientation), and neither-related cells (no significant correlation with the two factors).

The average firing rates of task-related cells and the former three classes of cells during CRT and MT were separately used as feather vectors for movement parameters decoding. The movement parameters conclude direction (2 classes), orientation (3 classes) and their combination (6 classes). The classifier based on k-nearest neighbor algorithm was employed offline. During different epochs, we randomly chose 20 groups of neurons from task-related cells and the former three classes of cells, with number of cells from 1 to 50, used for decoding and obtained the corresponding average decoding accuracy. From 108 trials of one set, 72 trials (2/3) formed the training set and the other 36 trials (1/3) formed the testing set.

We defined a cell's preferred movement direction and orientation based on its average firing rates during each epoch, which were averaged across all trials with the same direction or orientation. The preferred movement direction or orientation was the one with the highest average firing rate. We investigate the population of task-related cells, as well as cells related with direction or orientation during CRT and MT to check out their preference for direction and orientation respectively. Above signal analysis was implemented in MATLAB (Mathwork Inc.).

III. Results and Discussion

A. Cell Classification

A total number of 784 cells were sorted from 69 datasets in M1 of monkey Astra when it performed reach-to-grasp task. 425 (54.2%) of that showed task-related during movement planning stage (CRT), while 655 (83.5%) during movement execution stage (MT). Distribution of four categories of cells during the two epochs was shown in Fig. 2. We could find that from CRT to MT, the proportion of cells correlated with one factor only or both factors increases, which may suggest that more cells were recruited during movement execution to tune movement direction and target orientation. In addition, the significant increase of the proportion of orientation-only cells reflected that orientation was paid greater attention during movement execution.

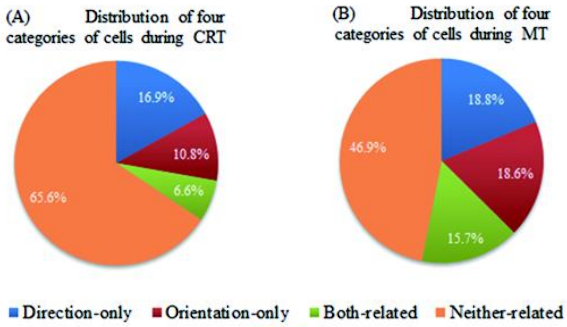

Figure 2. Distribution of four categories of cells during CRT (***A***) and MT (***B***).

B. Movement Parameters Decoding and Validity of Cell Classification

The average decoding accuracy of movement direction, orientation and combination of both parameters during MT and CRT was shown in Fig. 3. Task-related cells, both-related cells, direction-only cells and orientation-only cells during MT and CRT were respectively used for decoding. Since the numbers of both-related cells and orientation-only cells during CRT were below 50, we terminated it at the accessible maximal number of cells.

Decoding based on task-related cells during each epoch was regarded as a control group. The decoding performance of control group is not good enough in every subgraph. It may

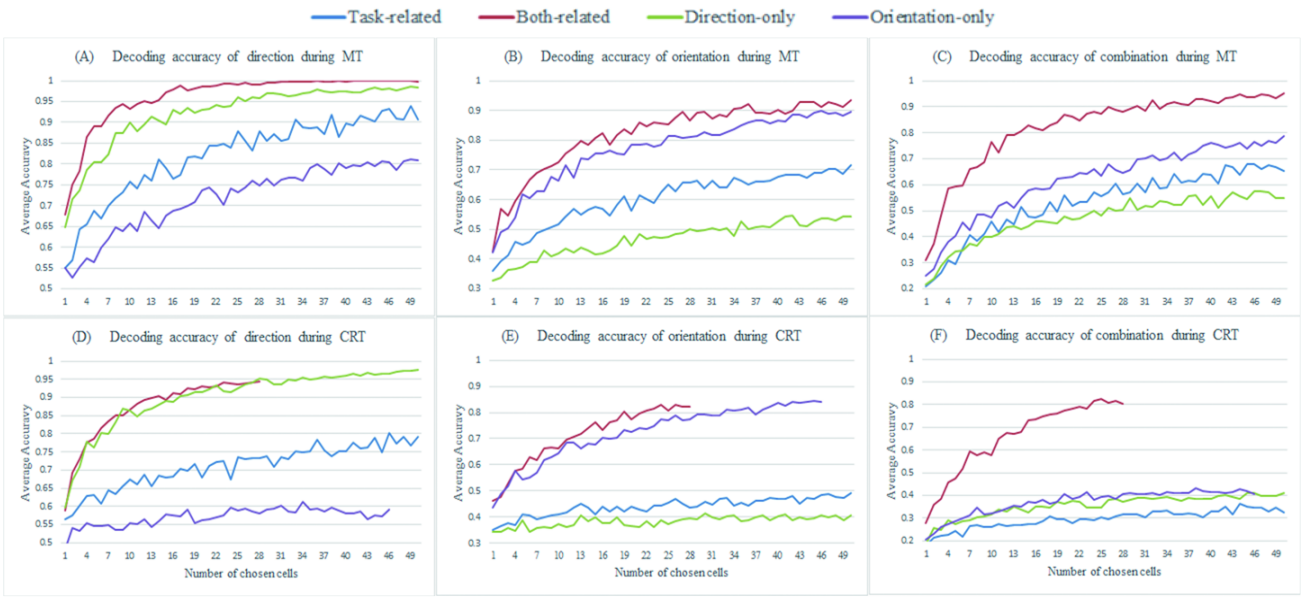

Figure 3. Average decoding accuracy of movement direction, orientation and combination of both parameters during MT *(A, B ,C)* and CRT *(D, E, F)*. Task-related cells, both-related cells, direction-only cells and orientation-only cells during MT and CRT were respectively used for decoding, corresponding to four different colors in every subgraph.

be because that there were lots of other parameters except for movement direction and orientation during the whole task and most cells were not related to the two parameter. If we perform decoding process based on the cell set containing a mixture of neither-related cells, the effect will be largely discounted. This inspires us choosing parameter-related cells to achieve better decoding accuracy and robustness.

Despite the small fluctuations, the average decoding accuracy increases with the number of neurons involved in decoding on the whole. Decoding based on both-related cells acquired the best performance no matter what parameter is decoded, during MT or CRT. In particular, when decoding the combination of both factors (Fig. 3C & 3F), the performance of both-related cells was far better than that of other cells. In practice, finding out both-related cells and using them for decoding could improve decoding accuracy, and meanwhile decrease the number of neurons involved.

Taken separately, when decoding movement direction (Fig. 3A & 3D) the direction-only cells did a pretty good job almost close to both-related cells, while the orientation-only cells performed worst, but when decoding target orientation (Fig. 3B & 3E) the contrary was the case. This suggested the importance of choosing cells from the appropriate categories which were related to the decoded parameters. The discrepancy between different classes of cells may be used to instruct decoding, and on the other hand, it also implied the validity of cell classification based on 2-way ANOVA.

C. *Role of M1 during Movement Planning*

We can see from Fig. 3 that for any parameter the average decoding accuracies during MT are much better than that during CRT. Intuitively, this is reasonable, because M1 has been universally acknowledged intimately related to movement execution, and it is premotor area which primarily involves in movement planning and orders movement commands to M1. On the other hand, even in the case of insufficient number of cells (only 28 both-related cells were found during CRT), the average decoding accuracies of parameters during CRT would exceed 80% (Fig. 3E & 3F), and even reach to 95% (Fig. 3D). This finding might suggest that M1 is more than a site accepting movement commands but also involves in movement planning.

Good decoding performance base on motor cortical activity during movement planning is of great significance for motor control of intelligent prostheses. Intelligent prostheses are designed mainly for people without motor ability or amputated, so it is natural that we should control the prostheses using signals of movement planning phase, before movement is actually performed.

D. *Comparison of three different classification algorithms*

Figure 4 shows the average decoding accuracy of combination of both movement direction and orientation during CRT and MT using both-related cells during respective epochs by three different algorithms: radial basis function (RBF) network, support vector machine (SVM) and KNN. We can see that no matter which epochs were used for decoding, SVM gets the best prediction accuracy. Even when using neural activity of only 25 both-related cells during CRT, the decoding accuracy by SVM is close to 90%. In comparison, KNN performs a little worse than SVM in respect to prediction accuracy, while its time consumption is far below that of SVM (Table 1). RBF performs the worst in both prediction accuracy and time consumption, which makes it out of an alternative choice for future application. It is worth noting that, with the increase of number of cells participating in decoding, the prediction accuracies of all three algorithms increase, while at the same time, the time consumption of SVM rises. It means that SVM obtains a good prediction accuracy at the sacrifice of time efficiency.

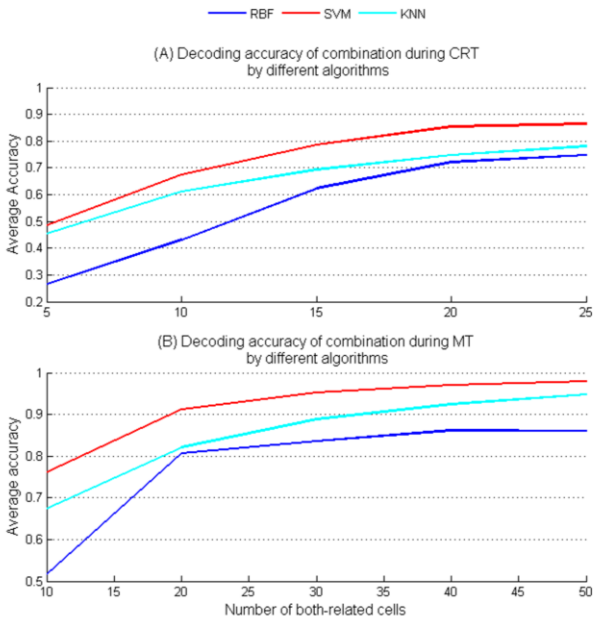

Figure 4. Average decoding accuracy of combination of both movement direction and orientation during CRT (A) and MT (B) using both-related cells during respective epochs by three different algorithms: RBF (blue), SVM (red) and KNN (blue-green).

TABLE I. RUN TIME OF THREE DIFFERENT CLASSIFICATION ALGORITHMS IN DECODING COMINATION DURING MT

Run Time (s)		Classification Algorithms		
		RBF	***SVM***	***KNN***
Number of chosen cells	10	45.38	18.01	0.01
	20	35.78	19.07	0.01
	30	35.00	20.70	0.01
	40	34.78	20.35	0.01
	50	32.97	23.83	0.01

IV. CONCLUSION

In the present study, we analyzed the neural signals of M1 in monkey Astra. According to the cells' correlation with movement direction and target orientation, we classified task-related cells during different epochs into four categories. Choosing enough number of cells from appropriate category and using their average firing rates as feature vectors of KNN classifier could actually improve the decoding accuracy. From another aspect, it also proves the validity of our cell classification principle. Particularly, the good decoding performance during movement planning, which is of great significance for intelligent prostheses control, also implies M1 more than accepting ready-made movement commands but also participating in movement planning. By contrast, SVM gets a better performance in terms of prediction accuracy since it has a higher generalization ability, but the training of support vector machine consumes such a long time that limits its application on real-time control. In further research, we would try to train and obtain a support vector machine with good generalization ability using fewer cells and fewer training samples, and apply it to the real-time tasks.

By far, we could just get a good decoding of movement parameters offline, while online decoding is more important for practical application and needs further study. Online decoding has a high requirement on the rapidity of decoding algorithm, so we adopted the simple, fast KNN algorithm as an attempt and achieved fairly good performance. On the other hand, here we used five independent microelectrodes for signal recording, each time we could only sort 7-19 neurons that is not enough for decoding. If a microelectrode array with more channels could be employed, we might be able to obtain a large number of cells at one time and decode the movement parameters pretty well.

ACKNOWLEDGMENT

This work is supported by National Natural Science Funds of China (60905024, 61233015), and 973 Project of China (2013CB329506). Sincerely thanks Dr. Jing Fan at Center of Neural Interface Design, ASU, for her contribution to the experiment.

REFERENCES

[1] Y. Guo and W. Li, "ENG-Based Signal Processing and Neural Decoding Algorithms for Rehabilitative Prostheses Control," in *Intelligent Human-Machine Systems and Cybernetics (IHMSC), 2013 5th International Conference on*, 2013, pp. 302-305.

[2] B. Reuderink, M. Poel, and A. Nijholt, "The impact of loss of control on movement BCIs," *Neural Systems and Rehabilitation Engineering, IEEE Transactions on,* vol. 19, pp. 628-637, 2011.

[3] L. R. Hochberg, M. D. Serruya, G. M. Friehs, J. A. Mukand, M. Saleh, A. H. Caplan*, et al.*, "Neuronal ensemble control of prosthetic devices by a human with tetraplegia," *Nature,* vol. 442, pp. 164-171, 2006.

[4] M. Velliste, S. Perel, M. C. Spalding, A. S. Whitford, and A. B. Schwartz, "Cortical control of a prosthetic arm for self-feeding," *Nature,* vol. 453, pp. 1098-1101, 2008.

[5] L. R. Hochberg, D. Bacher, B. Jarosiewicz, N. Y. Masse, J. D. Simeral, J. Vogel*, et al.*, "Reach and grasp by people with tetraplegia using a neurally controlled robotic arm," *Nature,* vol. 485, pp. 372-375, 2012.

[6] P. M. Rossini, S. Micera, A. Benvenuto, J. Carpaneto, G. Cavallo, L. Citi*, et al.*, "Double nerve intraneural interface implant on a human amputee for robotic hand control," *Clinical neurophysiology,* vol. 121, pp. 777-783, 2010.

[7] S. H. Scott, "The role of primary motor cortex in goal-directed movements: insights from neurophysiological studies on non-human primates," *Current opinion in neurobiology,* vol. 13, pp. 671-677, 2003.

[8] P. Cisek, D. J. Crammond, and J. F. Kalaska, "Neural activity in primary motor and dorsal premotor cortex in reaching tasks with the contralateral versus ipsilateral arm," *Journal of neurophysiology,* vol. 89, pp. 922-942, 2003.

[9] X. Lu and J. Ashe, "Anticipatory activity in primary motor cortex codes memorized movement sequences," *Neuron,* vol. 45, pp. 967-973, 2005.

[10] H.-C. Shin, V. Aggarwal, S. Acharya, M. H. Schieber, and N. V. Thakor, "Neural decoding of finger movements using Skellam-based maximum-likelihood decoding," *Biomedical Engineering, IEEE Transactions on,* vol. 57, pp. 754-760, 2010.

[11] W. Wu, M. J. Black, D. Mumford, Y. Gao, E. Bienenstock, and J. P. Donoghue, "Modeling and decoding motor cortical activity using a switching Kalman filter," *Biomedical Engineering, IEEE Transactions on,* vol. 51, pp. 933-942, 2004.

[12] J. Fan and J. He, "Motor cortical encoding of hand orientation in a 3-D reach-to-grasp task," in *Engineering in Medicine and Biology Society, 2006. EMBS'06. 28th Annual International Conference of the IEEE*, 2006, pp. 5472-5475.